CRACK STATISTIC OF CRYSTALLINE SILICON PHOTOVOLTAIC MODULES

M. Köntges[1], S. Kajari-Schröder[1], I. Kunze[1], U. Jahn[2]
[1]Institute for Solar Energy Research Hamelin (ISFH), Am Ohrberg 1, D-31860 Emmerthal, Germany
Tel: +49 5151 999 432; Fax: +49 5151 999 400; Email: Koentges@isfh.de
[2]TÜV Rheinland Energie und Umwelt GmbH, Solar Energy Assessment Center Cologne, Am Grauen Stein
51105 Köln, Germany

ABSTRACT: Solar cell cracks in wafer based silicon solar modules are a well-known problem. In order to identify the origin of cracks and thus lay the foundation for the inhibition of crack formation, we provide for the first time a statistic crack distribution in photovoltaic (PV) modules. We evaluate electroluminescence images of PV modules tested at the ISFH with respect to cracks. The results of the static load test and the "as delivered" PV modules are compared. Additionally we perform a simulation of the strain distribution on a glass plate subjected to a uniform mechanical load and supported at the edges, which is used as a measure for the relative mechanical load on the individual cells. The measured crack distribution correlates well with the stress distribution calculated by the simulation. "As delivered" PV modules show an average of 6% of broken cells per PV module. The analysis of the spatial distribution and orientation of micro cracks in PV modules offers valuable insight into the causes of micro cracks if the PV module is subject to a uniform mechanical load. It lays the foundation for PV module developments that reduce the risk of cracks, as well as for statistical power loss assessment.
Keywords: PV module, micro cracks, electroluminescence, lifetime

1 INTRODUCTION

Cracks in solar cells are a genuine problem for photovoltaic (PV) modules [1, 2, 3] as they are hard to avoid and, up to now, basically impossible to quantify in their impact on the efficiency of the module during its lifetime. In particular, the presence of micro cracks may have only a marginal effect on the power of a new module, as long as the different parts of the cells are still electrically connected. However, as the module ages and is subjected to thermal and mechanical stresses cracks may be introduced. A repeated relative movement of the cracked cell parts may result in a complete separation, thus resulting in inactive cell parts. For this special case a clear assessment of the power loss is possible. For a 60 cell 230 W PV module the loss of cell parts is acceptable as long the lost part is smaller than 8% of the cell area [4].

However up to now there is no statistical information on the distribution and the frequency of occurrence of micro cracks in the PV modules in literature. We aim to close this gap and provide a first statistic of cracks in PV modules for future power loss assessment and the development of crack inhibiting PV module concepts.

2 EXPERIMENTAL

For the analysis of cracks in PV modules we introduce crack pattern classes as shown in Tab. 1, which sort the cells according to the orientations of the cracks. Quite often the sorting of the cells into the bins is ambiguous. For example both a diagonal crack and a dendritic crack at a different position of the cell are present. Therefore the bins are prioritized, the priority of the bins decreasing from left to right in Table 1. Dendritic cracks could be considered to fall into the category of several crack directions (No. 2). However we decided to differentiate between these cracks because dendritic cracks indicate very high stress levels [5]. Note that the example for the perpendicular crack (No. 6) shows a cell whose backside busbar is only soldered on the right side of the cell. We decided to use this picture because it shows a well identifiable crack which is well suited for visualization purposes. Furthermore we choose to open up an extra bin (No. 7) for small cross cracks and cross crack lines because these types of cracks are introduced by very punctual stresses like support/measurement needles in the production or by scratching with a hard object across the module back sheet. Cross cracks are not initiated by transport or other surface loads and may occur unsystematically over the module.

Different crack orientations can have very different impact on the power output of PV modules. In particular, a single crack that leads to an electrical separation of a relevant part of the cell can significantly reduce the power output of a PV module [4, 6]. In contrast cracks that do not electrically separate cell parts only marginally affect the performance of a PV module [4]. In order to assess the criticality of the cracks we estimated the worst case impact of the different crack orientations in previous work [7]. The criticality of the crack concerning the PV module power loss is indicated by the roman numbers I = low criticality, II = moderate, III = high criticality in Tab. 1.

We choose to compare the crack distributions of just transported PV modules to PV modules exposed to a standard mechanical norm test. During a transport the

Tab. 1: Crack class bin definition for the crack sorting. The crack angle for the bins 3 to 6 may differ ±22.5° to the main bin angle.

0. No crack I	1. Dendritic crack III	2. Several directions III	3. +45° II	4. -45° II	5. Parallel to busbar III	6.Perp. to busbar I	7. Cross crack (line)II
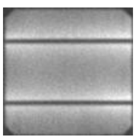		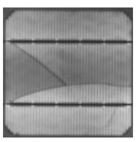	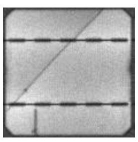	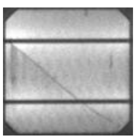	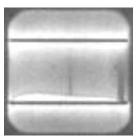	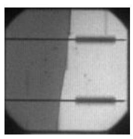	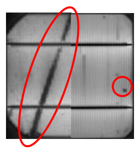

mechanical load for the PV module may have various causes. For example someone stands on the PV module package, the module oscillates caused by the transport vibrations or the PV module drops down because a module stack is picked up or set down to the ground a bit roughly. However the first eigenmode of the PV module vibration should occur in nearly all cases and should have the highest deflection compared to all other possible eigenmodes. The maximum deflection of the first eigenmode is similar to the defection form of a PV module exposed to a static homogeneous load. Therefore the crack distributions of the mechanical load and the more unknown transport load are expected to be similar.

Statistic of crack distribution of transported PV modules: The ISFH and TÜV Rheinland offer expert reports for PV modules to assess the quality of PV modules. For 83 (ISFH) and 20 (TÜV) of these reports electroluminescence (EL) images are taken and analysed with respect to crack orientations for the years 2008/9/10 and 11. The PV modules are from various manufactures with 60 multi or mono crystalline cells. Most of the PV modules are delivered in single module packages. The largest PV module package included into this investigation caries 5 PV modules. In all cases these PV modules were only transported from the manufacturer's location to the ISFH or TÜV Rheinland without being installed in the field. Within this work we do not know the initial state of the PV modules transported to the ISFH or TÜV. We explicitly accept that there are additional cracks which are not initiated by transport. PV modules with obvious indications for an exposure to a strong impact are sorted out. As indication for a strong impact we used the number of cells showing dendritic cracks. PV modules with more than one cell with dendritic cracks are sorted out. Fig. 2 shows an example image of a tumbled down PV module which vindicates this procedure. By a visual inspection no damage of the PV module can be seen. For all images and statistics shown in this work the junction box is always on the left hand side.

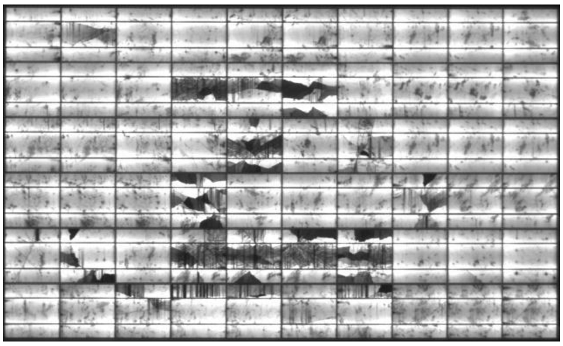

Fig. 2: Tumbled down PV module showing multiple dendritic cracked cells.

Statistic of crack distribution of PV modules tested by the IEC 61215 mechanical load test with 5400 Pa: The ISFH conducts mechanical load tests according to the standard IEC61215 with the 5400 Pa option. Before and after the test EL images are taken. With the help of digital image registration difference images are calculated to highlight the additional cracks due to the load test. Fig. 3 shows such a difference image. Red colour indicates regions, where the EL image is darker after the mechanical load test. Red crack like lines are counted as cracks introduced by the mechanical test. We perform the statistic analysis for twenty-seven 60 cell multi/mono crystalline PV modules. The modules are from various manufactures.

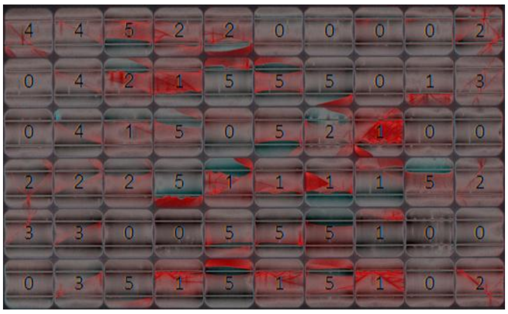

Fig. 3: EL images before and after the mechanical load are mapped to each other by the image registration method. Afterwards a difference image is calculated and colour coded. Red areas correspond to regions in the cells that appear darker in the EL after the load test, green areas indicate brighter regions and dark colour indicates no relevant change in EL intensity. The cell cracks are sorted manually into classes as explained in Tab. 1.

2.2 Experimental results

As a first step we look at the crack histogram of the as delivered PV modules in Fig. 4. We find that the percentage of modules with a specific number of cracks per PV module follows an exponential distribution for less than 6 cell cracks per PV module. For higher numbers of cracked cells the total number of PV modules per bin is too low for further analyses. However, 58% of the evaluated PV modules show 0 or 1 cracked cell, 28% of the PV modules have 2 to 5 cracked cells and about 14% show more than 5 cracked cells.

In a second step we compare the crack class distribution for the as delivered PV modules and the PV modules of the mechanical load test. As expected the total number of cracked cells is much higher for the PV modules of the mechanical load test (41%) compared to the as delivered PV modules (6%). Unfortunately the statistic of the as delivered solar modules is quite low despite of the high number of transported PV modules. Fig. 5 shows the results of crack class binning for both types of modules. In order to analyze the relative probability that a cell is cracked in a certain direction we define the relative crack class occurrence as the average occurrence per crack class relative to the total number of cracked cells.

The relative crack class occurrence differs for the as delivered and the mechanical loaded PV modules. There are only 354 cracked cells in total of the as delivered modules whereas the number of cracked cells after the mechanical load test is quite high resulting in 667 cracked cells. Due to the fact that we sorted all transported modules out with more than one dendritic cracked cell the number of dendritic cracked cells is quite low for the transported modules. From the mechanical point of view a dendritic cracked cell is similar to a cracked cell with several crack directions caused by a higher mechanical load. Putting this two classes together we find about 30% of all cells are cracked in several directions or dendritic independent of the chosen mechanical load. However the modules from the mechanical load test show a higher percentage of cells cracked parallel to the busbar than the as delivered modules. The perpendicular cracked cells are not important for both cases.

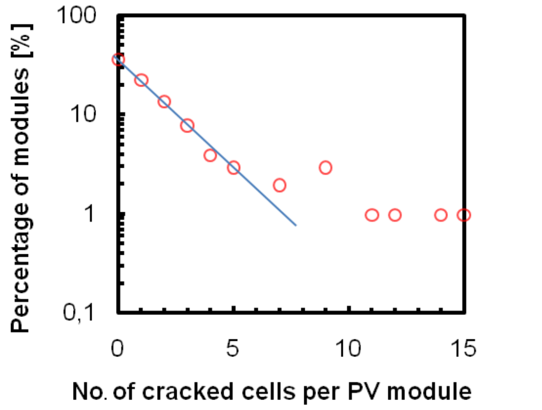

Fig. 4: Logarithmic histogram of PV modules showing a specific number of cracks per PV module. For low numbers of cracked cells an exponential distribution is found.

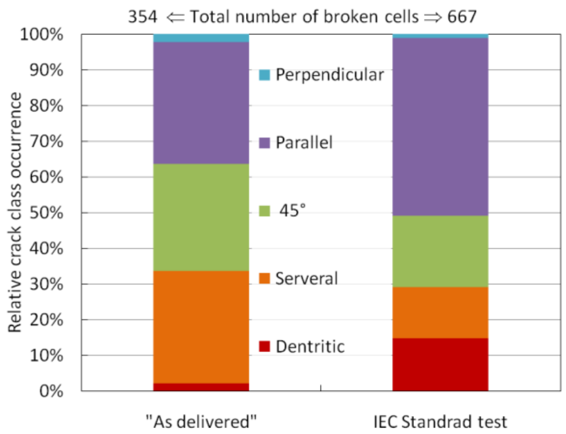

Fig.5: Comparison of the relative crack class occurrences of the "As delivered" and the mechanical load test. The "As delivered" PV modules show much less cracks parallel to the busbar.

We also analyze the spatial distribution of the cracks. Figures 6 and 7 depict the spatial distribution of the cracked cells for the transported modules and the mechanical load modules respectively. For the transported modules most of the cracks occur in the middle of the modules whereas in the mechanical load test the most cracked cells are located in the four corners and in the middle of the PV module. The statistical data is still quite noisy so that a clear signature of characteristic spatial distributions of crack probabilities cannot be identified. However, we enhance the visibility of spatial patterns by exploiting the two mirror symmetries of the PV module. The mechanical load is approximately uniform and thus also symmetric with respect to reaction along the two central axes. Figures 8 and 9 show the spatial distribution of cracking occurrence using the mirror symmetries of the PV module for the transported modules and the mechanical load test respectively. For cracks caused only by cell production and the stringing process one would expect a homogenous distribution. This is not the case. The statistical crack distribution shows significant local clusters.

3 SIMULATION OF STRAIN DISTRIBUTION

3.1 Simulation model

To understand the crack distribution we simulate a simplified model of a PV module. The answer of a PV module to mechanical loads is dominated by the properties of the glass as it is much thicker (3.2 mm) than the other materials. Therefore we model the PV module as a glass plate with the dimension (1 m x 1.6 m) of a typical 60 cell module. The frame of the PV module is implemented as boundary conditions prohibiting the displacement of the glass plate at the edges. On the one hand we perform an eigenfrequency analysis to simulate the conditions of the PV module transport. On the other hand we introduce a surface pressure load of 5400 Pa to the top of the glass plate to simulate the test conditions of the mechanical load test. The strain calculated at the bottom surface of the plate is a measure for the strain of the solar cells laminated to the glass. The resulting strain is compared to the crack statistic derived from both mechanical loads described above.

3.2. Simulation results

The simulated first eigenfrequency is about 11 Hz for the PV module sized glass plate. This result is consistent with the first eigenfrequency found experimentally by another group being in the range of 5 to 11 Hz [8]. The simulated relative first principle strain is shown in Fig. 8 and 9 in the image named "simulation". Both simulations show a high first principle strain in the middle of the PV module and along the diagonal. The main difference between the strain distribution for the eigenfrequency analysis and the static load is found in the PV module corners. The eigenfrequency analysis shows a lower strain in the corners relative to the strain in the middle compared to the simulated static load. All other characteristics, especially the first and second principle strain, are quite similar.

R/C	1	2	3	4	5	6	7	8	9	10
1	3	8	7	3	4	6	6	4	5	2
2	6	4	9	9	10	9	10	9	7	4
3	3	7	7	6	6	10	9	5	3	6
4	4	2	6	7	8	3	4	3	3	5
5	5	8	8	9	7	8	13	6	6	5
6	2	6	7	5	8	3	3	6	5	3

Fig. 6: Statistical distribution of cracks for transported PV modules. Each field represents a cell position and the number is the percentage of cells cracks at that position.

R/C	1	2	3	4	5	6	7	8	9	10
1	59	37	37	41	26	41	33	52	33	63
2	11	48	59	44	44	41	44	44	52	22
3	22	30	48	37	33	52	26	37	33	26
4	33	26	41	33	52	33	44	33	37	41
5	44	59	41	26	59	41	70	67	48	30
6	52	33	41	56	41	37	22	44	44	63

Fig. 7: Statistical distribution of cracks for PV modules loaded in accordance to standard IEC61215 with the 5400 Pa option. Each field represents a cell position and the number is the percentage of cells cracks at that position.

Cracked cells [%]

R/C	1	2	3	4	5
1	2	6	6	4	5
2	5	6	8	10	8
3	4	4	5	6	7

Dentritic cracks [%]

R/C	1	2	3	4	5
1	0	0	0	0	0
2	0	0	0	0	0
3	0	0	0	0	0

Serveral directions [%]

R/C	1	2	3	4	5
1	1	1	1	0	1
2	0	2	2	4	2
3	1	1	2	3	1

Cells per module:	60
Number of modules:	103
Cracked cells per module[%]:	5,74
Cracked cells per module[#]:	3,45

Parallel to Busbar [%]

R/C	1	2	3	4	5
1	0	1	1	2	2
2	1	0	2	3	4
3	1	1	1	1	2

Perpendicular to Busbar [%]

R/C	1	2	3	4	5
1	0	0	0	0	0
2	0	0	0	0	0
3	0	0	0	0	0

45° cracks [%]

R/C	1	2	3	4	5
1	0	2	1	0	0
2	1	2	2	1	0
3	0	1	3	0	1

Simulation approx. 11 Hz

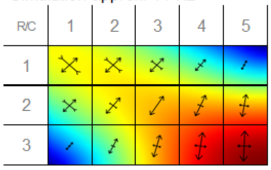

Fig. 8: Statistical distribution of cell crack directions for transported PV modules. Using the horizontal and vertical symmetry equal cell positions are mapped to one position. The simulation shows a colour coded maximum strain diagram in arbitrary units of the bottom surface of a glass plate for the first eigenmode of a glass plate. The arrows show the direction and amplitude of the first and second principle strain.

Cracked cells [%]

R/C	1	2	3	4	5
1	59	37	44	38	36
2	27	52	53	46	46
3	31	31	40	35	43

Dentritic cracks [%]

R/C	1	2	3	4	5
1	5	1	2	2	3
2	9	9	6	6	10
3	11	4	8	6	10

Serveral directions [%]

R/C	1	2	3	4	5
1	6	2	3	3	1
2	5	9	10	4	1
3	8	6	14	6	11

Cells per module:	60
Number of modules:	27
Cracked cells per module[%]:	41,2
Cracked cells per module[#]:	24,7

Parallel to Busbar [%]

R/C	1	2	3	4	5
1	0	19	35	32	32
2	1	18	30	33	33
3	4	12	15	22	21

Perpendicular to Busbar [%]

R/C	1	2	3	4	5
1	0	0	0	0	0
2	1	0	0	0	0
3	6	0	0	0	0

45° cracks [%]

R/C	1	2	3	4	5
1	48	15	4	0	0
2	10	16	6	3	1
3	1	5	11	1	0

Simulation pressure 5400 Pa

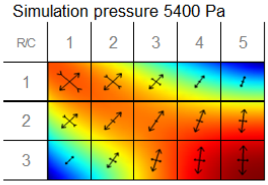

Fig. 9: Statistical distribution of cell crack directions for PV modules loaded in accordance to standard IEC61215. Using the horizontal and vertical symmetry equal cell positions are mapped to one position. Each field represents a cell position. The field number is the percentage of cell cracks at that position. The simulation shows a colour coded strain diagram in arbitrary units of the bottom surface of a glass plate under a static load of 5400 Pa. The arrows show the direction and amplitude of the first and second principle strain.

4 DISCUSSION

The histogram of the number of cracked cells per module depicted in Fig. 4 may be interpreted as two different types of distributions. The very well fitting exponential distribution for low numbers of cracked cells (≤ 5) may be caused by an intrinsic failure mechanism. For us it is a bit surprising that PV modules of so many different manufactures and transportation concepts result in such a clear exponential distribution. The individual PV modules with high numbers of cracked cells may be caused by a special but common event, for example a high mechanical load during transport. However the number of modules with more than 5 cracked cells is too low for a more precise analysis.

The comparison of the numerically calculated strain and the statistical analysis of the crack occurrence in PV modules after transport and after mechanical load test shows good qualitative agreement, which we discuss in detail in the following. Especially the relative number of cracked cells and of the cells cracked in several directions correlate with the highest strain of the simulations. Both tests differ very much in the intensity of the mechanical load. In fact we do not know the maximum load introduced during the transport of the modules but we learn from the number of broken cells (6%) that the intensity of the mechanical load must be much smaller than during the mechanical load test (41%).

The difference found between the two simulations concerning the PV module corners is found to be very pronounced in the experiment. In the experiment the transported modules show only a small amount of broken cells in the corners whereas the PV modules of the mechanical load test show a very high number of broken cells in the corners.

Both simulations give quite similar strain distributions. However the statistical distribution of the crack directions in Fig. 5 shows that cracks parallel to the busbar occur more often in the static load test compared to the as delivered PV modules. From the simulated strain distribution we should expect nearly the same amount of parallel cracked cells. We see also that the some cracks parallel to the busbar are located in regions with relative low strain. As discussed before we assume that the as delivered cells have been exposed to a much lower mechanical load than those during the IEC test. Thus, the threshold for occurrence of cracks may avoid that cracks occur at low loads.

The percentage of cracked cells per position qualitatively matches to the amplitude of the first principle strain at each position for both load cases. Furthermore the experiments show a correlation between the first principle strain direction and the crack direction. For example the crack probability for busbar parallel cracks is high if the direction of the first principle strain is perpendicular to the busbars. Furthermore diagonal cracks have a high probability at locations of first principle strain perpendicular to the diagonal. These correlations do not hold where the second principle strain is a tensile non small value. This is the case in the middle of the module. But especially at these positions the crack type “several crack directions” has a high probability.

5 CONCLUSIONS

In our experiments we find that the distribution of cracks in as delivered PV modules shows a spatial distribution similar to the strain distribution of the first eigenmode of the front glass plate. We conclude that the mechanical loads during the transportation is the most important cause for the crack growth in PV-modules. A crack itself has no significant impact on the power of a PV module. But the crack orientation determines the criticality of a crack. Therefore a test procedure for PV modules has to take this into account. PV modules should first experience mechanical load testing followed by some thermo cycling testing to evaluate power loss due to the crack propagation.

Furthermore the handling and transport of a PV module should be reconsidered to reduce mechanical loads to a PV module as much as possible. The predominant crack classes are “cells with more than one crack direction” and “cracks parallel to the busbar”. Especially the cracks parallel to the busbar may degrade the module power most. For new PV module designs the preferred crack orientation should be taken into account to prevent the PV module from power loss. One simple change in design is to rotate the solar cells in the PV module by 90° to change the criticality of the predominant crack direction.

Up to now there is not much experience with power loss due to cracked cells in PV modules from the field. But the results from previous work show that accelerated aging tests from pre-cracked cells may lead to power loss. In average 6% of the cells of as delivered PV module do have a crack.

6 ACKNOWLEDGEMENTS

Funding was provided by the State of Lower Saxony and the German Federal Ministry for the Environment, Nature Conservation, and Nuclear Safety (BMU) under contract no. 0325194C (Task 13).

7 REFERENCES

[1] S. Pingel, Y. Zemen, O. Frank, T. Geipel and J. Berghold, Mechanical stability of solar cells within solar panels, Proc. of 24th *EUPVSEC* (WIP, Dresden, Germany, 2009) 3459-3464

[2] A. M. Gabor, M. M. Ralli, L. Alegria, C. Brodonaro, J. Woods, L. Felton, 21st EU PVSEC (Dresden, Germany, 2006) 2042-2047

[3] M. Köntges, K. Bothe, Photovoltaik Aktuell supplement in Elektro Praktiker 7/8 2008, p. 36-40

[4] M. Köntges, I. Kunze, S. Kajari-Schröder, X. Breitenmoser, B. Bjørneklett, Sol. Energy Mater. Sol. Cells (2011), doi:10.1016/ j.solmat.2010.10.034

[5] S. Kajari-Schröder, I. Kunze, U. Eitner, M. Köntges, 26th Symposium Photovoltaische Solarenergie (OTTI, Bad Staffelstein, Germany, 2011), p. ???

[6] P. Grunow, P. Clemens, V. Homann, B. Litzenburger, L. Podlowski, Proc. of 20th EU PVSEC (Barcelona, Spain,2005) 5BV.4.26

[7] S. Kajari-Schröder, I. Kunze, U. Eitner, M. Köntges, Sol. Energy Mater. Sol. Cells (2011),doi: 10.1016/j.solmat.2011.06.032

[8] F. Reil, W. Hermann, U. Jahn, Bruchcharakteristik von kristallinen PV-Modulen unter mechanischer Belastung und deren Einfluss auf das elektrische Verhalten“. 25th Symposium Photovoltaische Solarenergie,(OTTI, Bad Staffelstein, Germany, 2010), p. 476